Gα$_{12}$ Structural Determinants of Hsp90 Interaction Are Necessary for Serum Response Element–Mediated Transcriptional Activation

Ellyn R. Montgomery, Brenda R. S. Temple, Kimberly A. Peters, Caitlin E. Tolbert, Brandon K. Booker, Joseph W. Martin, Tyler P. Hamilton, Alicia C. Tagliatela, William C. Smolski, Stephen L. Rogers, Alan M. Jones, and Thomas E. Meigs

Department of Biology, University of North Carolina at Asheville, Asheville, North Carolina (E.R.M., B.K.B., J.W.M., T.P.H., A.C.T., W.C.S., T.E.M.); Departments of Biology (K.A.P., S.L.R., A.M.J.), Biochemistry and Biophysics (B.R.S.T.), Cell Biology and Physiology (C.E.T.), and Pharmacology (A.M.J.), R. L. Juliano Structural Bioinformatics Core Facility (B.R.S.T.), and Carolina Center for Genome Sciences (S.L.R.), University of North Carolina, and the Lineberger Comprehensive Cancer Center, (S.L.R., T.E.M.), Chapel Hill, North Carolina

Received July 17, 2013; accepted January 16, 2014

ABSTRACT

The G12/13 class of heterotrimeric G proteins, comprising the α-subunits Gα$_{12}$ and Gα$_{13}$, regulates multiple aspects of cellular behavior, including proliferation and cytoskeletal rearrangements. Although guanine nucleotide exchange factors for the monomeric G protein Rho (RhoGEFs) are well characterized as effectors of this G protein class, a variety of other downstream targets has been reported. To identify Gα$_{12}$ determinants that mediate specific protein interactions, we used a structural and evolutionary comparison between the G12/13, Gs, Gi, and Gq classes to identify "class-distinctive" residues in Gα$_{12}$ and Gα$_{13}$. Mutation of these residues in Gα$_{12}$ to their deduced ancestral forms revealed a subset necessary for activation of serum response element (SRE)–mediated transcription, a G12/13-stimulated pathway implicated in cell proliferative signaling. Unexpectedly, this subset of Gα$_{12}$ mutants showed impaired binding to heat-shock protein 90 (Hsp90) while retaining binding to RhoGEFs. Corresponding mutants of Gα$_{13}$ exhibited robust SRE activation, suggesting a Gα$_{12}$-specific mechanism, and inhibition of Hsp90 by geldanamycin or small interfering RNA–mediated lowering of Hsp90 levels resulted in greater downregulation of Gα$_{12}$ than Gα$_{13}$ signaling in SRE activation experiments. Furthermore, the *Drosophila* G12/13 homolog Concertina was unable to signal to SRE in mammalian cells, and Gα$_{12}$:Concertina chimeras revealed Gα$_{12}$-specific determinants of SRE activation within the switch regions and a C-terminal region. These findings identify Gα$_{12}$ determinants of SRE activation, implicate Gα$_{12}$:Hsp90 interaction in this signaling mechanism, and illuminate structural features that arose during evolution of Gα$_{12}$ and Gα$_{13}$ to allow bifurcated mechanisms of signaling to a common cell proliferative pathway.

Introduction

The ability to perceive and respond to information from the environment is a fundamental property of living cells. G protein–coupled receptors (GPCRs) are integral membrane proteins that evolved to detect a wide range of extracellular signals, including neurotransmitters, hormones, odorants, and light. On activation, GPCRs undergo a conformational change that stimulates heterotrimeric G proteins, intracellular

signaling molecules that consist of a GTP-binding α-subunit that exists in 1:1:1 stoichiometry with a β- and a γ-subunit. This heterotrimer is inactive when Gα is GDP-bound and GPCR activation causes Gα to exchange GDP for GTP, dissociate from the Gβγ heterodimer, and activate downstream effector proteins (Oldham and Hamm, 2008). Gα proteins are categorized into four classes based on amino acid sequence: Gs, Gi, Gq, and G12/13. Although each class signals to distinct effector proteins, Gα proteins share a common fold; thus, it is widely accepted that Gα–effector interactions are dictated by class-specific amino acids that create permissive binding surfaces (Cabrera-Vera et al., 2003). Understanding the principles that govern Gα–effector interaction is essential to deciphering the role of specific signaling pathways.

The G12/13 class of Gα proteins is involved in signaling networks that regulate cell migration, cytoskeletal rearrangements,

ABBREVIATIONS: EGFP, enhanced green fluorescent protein; GFP, green fluorescent protein; GPCR, G protein–coupled receptor; GST, glutathione-*S*-transferase; HEK, human embryonic kidney; Hsp90, heat-shock protein 90; IRES, internal ribosomal entry site; LARG, leukemia-associated RhoGEF; MRTF, myocardin-related transcription factor; PBS, phosphate-buffered saline; PCR, polymerase chain reaction; RBD, Rho-binding domain; RhoGEF, guanine nucleotide exchange factor for Rho; siRNA, small interfering RNA; SRE, serum response element.

adhesion, apoptosis, and growth (Juneja and Casey, 2009; Suzuki et al., 2009). Consistent with their role as signaling hubs in these pathways, overexpressed or constitutively activated Gα$_{12}$ and Gα$_{13}$ are potent stimulators of oncogenic transformation (Chan et al., 1993; Jiang et al., 1993; Xu et al., 1994). Some of these responses appear to involve transcriptional activation of growth-promoting genes governed by promoters harboring the serum response element (SRE) (Vara Prasad et al., 1994; Hill et al., 1995; Fromm et al., 1997). Other responses point to cell migration: endogenous Gα$_{12}$ levels correlate with the degree of metastatic invasiveness in breast cancer tissue samples (Kelly et al., 2006a), and androgen-insensitive, invasive prostate tumor cells exhibit higher Gα$_{12}$ levels than less aggressive prostate cancers (Kelly et al., 2006b). Despite 65% amino acid identity, Gα$_{12}$ and Gα$_{13}$ have nonoverlapping roles in signaling, embryonic development, and disease physiology. Mice lacking Gα$_{13}$ exhibit embryonic lethality with impairment in vascular development (Offermanns et al., 1997), whereas mice lacking Gα$_{12}$ appear to develop normally (Gu et al., 2002). However, in mice that are haplo-insufficient for Gα$_{13}$, at least one wild-type allele of Gα$_{12}$ is required to avoid lethality (Worzfeld et al., 2008), suggesting that Gα$_{12}$ function during development is not eclipsed by Gα$_{13}$. Also, studies of mouse embryonic fibroblasts lacking Gα$_{12}$ and Gα$_{13}$ reveal that both proteins are necessary for orientation of the microtubule-organizing center (Goulimari et al., 2008).

The mechanisms through which Gα$_{12}$ and Gα$_{13}$ stimulate cell proliferation are not well understood. The best characterized effector proteins are Rho-specific guanine nucleotide exchange factors (RhoGEFs) that interact with Gα$_{12}$ and Gα$_{13}$ via RGS (regulator of G protein signaling) homology domains; these include p115RhoGEF, leukemia-associated RhoGEF (LARG), and PDZ-RhoGEF (Sternweis et al., 2007). In addition to regulating cytoskeletal events such as contraction, this G12/13-RhoGEF-Rho axis also stimulates transcription through the SRE, a promoter element of the c-fos protooncogene (Fromm et al., 1997; Bhattacharyya and Wedegaertner, 2000; Shi et al., 2000). This signaling event is mediated by the transcriptional activator serum response factor, which itself requires Rho-mediated nuclear translocation of its cofactor, myocardin-related transcription factor-A (MRTF-A) (Wang et al., 2002). Although Gα$_{12}$ and Gα$_{13}$ signal through several common binding partners, numerous studies provide evidence of selectivity within the G12/13 class (Kelly et al., 2007). For example, activity of heat-shock protein 90 (Hsp90) is required for Gα$_{12}$, but not Gα$_{13}$, to stimulate cellular transformation (Vaiskunaite et al., 2001). Hsp90 is a molecular chaperone that forms a homodimer in the cytoplasm, and hydrolysis of ATP at N-terminal binding pockets within this dimer facilitates engagement and stabilization of a wide variety of Hsp90 client proteins, many of which are implicated in cancer progression (Samant et al., 2012). Hsp90 binds specifically to Gα$_{12}$ within the G12/13 class, but the structural features that mediate this interaction are unknown.

Recent studies used a taxonomic comparison of Gα proteins to identify changes in key residues that contributed to the evolutionary diversification of the four classes (Friedman et al., 2009; Temple et al., 2010). In the present study, we mutated "class-distinctive" residues in Gα$_{12}$ to ancestral forms to dissect their roles in distinct signaling pathways. Our results revealed a subset of these class-distinctive mutations

in Gα$_{12}$ that disrupted both SRE activation and Hsp90 binding. Gα$_{13}$ variants harboring identical mutations displayed robust SRE activation, suggesting a Gα$_{12}$-specific mechanism. In addition, the *Drosophila* G12/13 homolog Concertina was unable to drive SRE signaling when expressed in mammalian cells, and subsequently we used this protein as a platform to identify key determinants of growth signaling in the switch regions and C-terminal region of Gα$_{12}$. These findings define Gα$_{12}$-specific structural determinants of SRE activation and implicate Hsp90 binding as a requirement for this Gα$_{12}$-mediated pathway.

Materials and Methods

Materials and DNA Constructs. Glutathione-S-transferase (GST) fusions of the N-terminal 252 amino acids of p115RhoGEF and the region spanning Leu320 to Arg606 of LARG were provided by Tohru Kozasa (University of Illinois, Chicago) and have been described previously (Meigs et al., 2005). A GST fusion of the C-terminal 107 amino acids of Hsp90-α was provided by Tatyana Voyno-Yasenetskaya (University of Illinois, Chicago), and enhanced green fluorescent protein (EGFP)–fused MRTF-A was a gift from Christopher Mack (University of North Carolina, Chapel Hill). All point mutants of Gα$_{12}$, Gα$_{13}$, and Concertina were engineered by oligonucleotide-directed mutagenesis using the QuikChange II system (Agilent Technologies, Englewood, CO), with the following exception to the manufacturer's instructions. Each initial amplification reaction was divided into equal halves, with each receiving one of two mutagenic oligonucleotides for the first two polymerase chain reaction (PCR) cycles. These half-reactions were then combined and subjected to 15 additional PCR cycles. Concertina mutants in the internal ribosomal entry site (IRES) vector pLL-5.5 (Uetrecht and Bear, 2009) were engineered by first excising the Concertina cDNA from pLL-5.5 using ApaI and EcoRI, subcloning into a truncated pGEX-2T vector (GE Healthcare, Little Chalfont, Buckinghamshire, UK) at these sites and then using QuikChange II reagents to introduce codon substitutions. Mutants were subcloned into pLL-5.5 and then confirmed by sequencing. To introduce myc-Gα$_{12}$^{QL} to pLL-5.5, we excised the Concertina cDNA from pLL-5.5 by digesting with ClaI, blunting 5′-overhangs with Klenow and digesting with EcoRI. Next, myc-Gα$_{12}$^{QL} cDNA was excised from pcDNA3.1 (Life Technologies, Grand Island, NY), using EcoRI and the blunt end-generating PmeI, and was ligated into pLL-5.5. All DNA constructs expressed in *Drosophila* cell culture were subcloned into a metallothionein promoter, pmtA vector backbone (Life Technologies), and a myc epitope tag was introduced N-terminally after the initiator Met using KOD Xtreme Hot Start Polymerase (EMD Millipore, Billerica, MA). All Gα$_{12}$/Concertina and Gα$_{13}$/Concertina chimeras were engineered by a two-step PCR procedure, in which desired regions of the mutationally activated Gα$_{12}$ (Q229L), Gα$_{13}$ (Q226L), and Concertina (Q303L) cDNAs were amplified so that each initial product contained an additional nine base pairs that overlapped with the product amplified from the other cDNA. This created junctions in which 18 base pairs formed, allowing the initial PCR products (two for chimeras 1, 2, 3, and 4, three for all other chimeras) to be combined with end primers in a second round of PCR cycling to generate a full chimeric product. For N-terminal tagging of chimeras 3, 4, 5, and 4-sub, the coding sequence was amplified by PCR with the myc epitope tag EQKLISEEDL encoded in the forward primer immediately downstream of the initiator methionine, and each product was subcloned into pcDNA3.1+ (Life Technologies). All constructs were verified by sequencing.

Expression and Immobilization of GST Fusion Proteins. The GST fusion constructs were transformed into BL21(Gold)-DE3 cells (Agilent Technologies), liquid cultures were grown at 37°C under 75 μg/ml ampicillin selection to OD$_{600}$ of 0.5–0.7, and recombinant protein expression was induced by 0.5 mM isopropyl-β-D-thiogalactopyranoside

(Fisher Scientific, Pittsburgh, PA). After 3 hours, the cells were lysed on ice using 0.32 mg/ml lysozyme (MP Biomedicals, Santa Ana, CA), and GST fusion proteins were bound to glutathione Sepharose 4B (GE Healthcare) as described previously (Meigs et al., 2005). After three washes in 50 mM Tris pH 7.7 supplemented with 1 mM EDTA, 1 mM dithiothreitol, and 150 mM NaCl, samples were snap-frozen and stored at -80°C.

Preparation of Detergent-Soluble Extracts Harboring Gα Mutants. Human embryonic kidney cells (HEK293) were grown in Dulbecco's modified Eagle's medium (Mediatech, Manassas, VA) supplemented with 10% fetal bovine serum (Hyclone, Logan, UT), penicillin, and streptomycin. For myc-Gα_{12}^{QL} and each of the class-distinctive mutants, 7.0 μg of plasmid DNA was transfected into a 10-cm dish of HEK293 cells at approximate 90% confluence, using Lipofectamine 2000 (Invitrogen) in accordance with the manufacturer's instructions. After 36–40 hours, cells were scraped from dishes, washed twice with phosphate-buffered saline (PBS), and solubilized in lysis buffer [50 mM HEPES pH 7.5, 1 mM EDTA, 3 mM dithiothreitol, 10 mM MgSO$_4$, 1% (w/v) polyoxyethylene-10-lauryl ether] containing the protease inhibitors 4-(2-aminoethyl)benzenesulfonyl fluoride hydrochloride (1.67 mM), leupeptin (2.1 μM), pepstatin (1.45 μM), Nα-tosyl-L-lysine chloromethyl ketone (58 μM), tosyl-L-phenylalanyl-chloromethane (61 μM), and phenylmethylsulfonyl fluoride (267 μM). Samples were centrifuged at 80,000g for 1 hour, and supernatants were snap-frozen and stored at -80°C.

Trypsin Protection Assays. HEK293 cells grown in 10-cm dishes were transfected with various Gα_{12} constructs using Lipofectamine 2000, and tryptic digestions were performed as a modification of the procedure of Kozasa and Gilman (1995). Briefly, cells were lysed in 50 mM HEPES, pH 7.5, 1 mM EDTA, 3 mM dithiothreitol, and 1% polyoxyethylene-10-lauryl ether containing the same protease inhibitors as lysis buffer (see preceding) but at 2-fold lower concentration. Samples were cleared by centrifugation at 80,000g for 1 hour, and supernatants were diluted 20-fold in volume using 50 mM HEPES pH 7.5, 1 mM EDTA, 3 mM dithiothreitol, and 10 mM MgSO$_4$. Samples were digested with 10 μg/ml TPCK-treated trypsin (New England Biolabs, Ipswich, MA) for 20 minutes at 30°C, and proteolysis was terminated by addition of 100 μg/ml lima bean trypsin inhibitor (Worthington, Lakewood, NJ). Proteins were precipitated by addition of 20% trichloroacetic acid and 0.8 mg/ml sodium deoxycholate, washed with acetone, dried, and then analyzed by SDS-PAGE and immunoblotting using J169 antisera specific to the Gα_{12} C terminus (Kozasa and Gilman, 1995), provided by Tohru Kozasa (University of Illinois, Chicago).

Protein Interaction Assays. Extracts from transfected HEK293 cells were diluted in lysis buffer (see preceding description) lacking polyoxyethylene-10-lauryl ether, using sufficient volume to dilute this detergent to 0.05% (w/v). Next, Sepharose-bound GST fusion proteins were added and continuously inverted for 2 hours at 4°C. A percentage of the diluted extract was set aside as starting material (i.e., load) before Sepharose addition. Samples were centrifuged at 1,300g, and pellets were washed extensively and subjected to SDS-PAGE and immunoblot analysis using an antibody specific to either the Gα_{12} N terminus (Santa Cruz Biotechnology, Santa Cruz, CA), Gα_{13} (EMD Millipore), or the myc epitope tag (EMD Millipore), followed by alkaline phosphatase conjugated secondary antibodies (Promega, Madison, WI). For each Gα protein, the Gaussian intensity value was determined for the ~44-kDa band in the precipitated material and divided by the Gaussian intensity of the corresponding ~44 kDa-band in the load to normalize Gα variants for different expression levels in cells.

RhoA Activity Assays. Pull-downs using the Rho-binding domain (RBD) of Rhotekin were performed as previously described (Ren et al., 1999) with the following minor modifications. Cells were washed with ice-cold Tris buffered saline (pH 7.6) with 2 mM MgCl$_2$ and lysed in buffer A (50 mM Tris pH 7.6, 500 mM NaCl, 1% Triton X-100, 0.1% SDS, 0.5% sodium deoxycholate, 0.5 mM MgCl$_2$, 200 μM orthovanadate, 10 μg/ml aprotinin, 10 μg/ml leupeptin, 1 mM

phenylmethylsulfonyl fluoride). Lysates were sonicated briefly, clarified by centrifugation, and equalized for total volume, as well as protein concentration, and then incubated with 30 μg of GST-RBD beads prepared as previously described (Guilluy et al., 2011). Samples were washed with buffer B (50 mM Tris pH 7.6, 150 mM NaCl, 1% Triton X-100, 0.5 mM MgCl$_2$, 200 μM orthovanadate, and protease inhibitors as described) three times before SDS-PAGE. Active RhoA, total RhoA, Gα_{12}, and actin levels were determined by immunoblotting with anti-RhoA (polyclonal antibody 67B9; Cell Signaling Technology, Danvers, MA), anti-Gα_{12} (Santa Cruz Biotechnology), and anti-actin (clone C4; EMD Millipore). Total RhoA and Gα_{12} levels were similarly determined using an aliquot of whole cell lysate.

Reporter Gene Assays and RNA Interference. SRE-luciferase plasmid was provided by Channing Der (University of North Carolina, Chapel Hill). HEK293 cells grown to approximately 80% confluence in 12-well plates were transfected with 0.2 μg of SRE-luciferase and 0.02 μg pRL-TK harboring the cDNA for *Renilla* luciferase (Promega), plus 1.0 μg plasmid encoding a variant of myc-Gα_{12}^{QL}, Gα_{13}^{QL}, or Concertina. Plasmid mixtures were combined with Lipofectamine 2000 in Opti-MEM reduced serum medium (Life Technologies) according to the manufacturer's instructions. For RNA interference experiments, small interfering RNA (siRNA) specific to Hsp90-α (ON-TARGETplus SMARTpool; Thermo Scientific Dharmacon, Pittsburgh, PA) was reconstituted in 1× siRNA buffer (Thermo Scientific Dharmacon), and 60 pmol per sample was combined with the plasmids described above and cotransfected using Lipofectamine 2000 into 12-well plates of HEK293 cells. Assays for SRE activation were performed as described previously (Meigs et al., 2005). Briefly, cells were washed with phosphate-buffered saline and lysed in 1× passive lysis buffer (Promega), and lysates were analyzed using a Dual-luciferase assay system and GloMax 20/20 luminometer (Promega). Light output from firefly luciferase activity was divided by output from *Renilla* luciferase activity to normalize for variations in transfection efficiency.

Visualization of MRTF-A Localization. Subcellular distribution of EGFP-tagged MRTF-A was assayed as previously reported (Hinson et al., 2007; Medlin et al., 2010) with minor modifications. HEK293 cells grown on glass coverslips to approximately 50% confluence were transfected with plasmids encoding EGFP-MRTF-A and variants of Gα_{12} using Lipofectamine 2000 (Life Technologies). After 36 hours, cells were washed in PBS and fixed in 4% paraformaldehyde for 10 minutes, rinsed three times in PBS, and mounted on 4′,6-diamidino-2-phenylindole–Fluoromount-G (Southern Biotech, Birmingham, AL). Cells were visualized on a TE-2000S (Nikon, Melville, NY) equipped with a SPOT monochrome digital camera (Diagnostic Instruments, Sterling Heights, MI). Individual cells were examined for 4′,6-diamidino-2-phenylindole fluorescence to define the nuclear compartment, followed by green fluorescence to visualize EGFP-MRTF-A distribution.

***Drosophila* Cell Culture and Imaging.** S2 cells were obtained and cultured as previously described (Rogers and Rogers, 2008). Cells were maintained in SF900 media (Life Technologies) and were transfected with 2 mg/ml DNA using the Amaxa nucleofector system (Lonza, Basel, Switzerland) with KitV and program G-30. Cells were plated onto ConA-coated coverslips in petri dishes and induced with 1 mM CuSO$_4$ for 2.5 hours. Cells were prepared for imaging as previously described (Rogers and Rogers, 2008). Probes used were 1:400 diluted anti-myc (9E10) antibody (DSHB, Iowa City, IA) and 1:100 diluted Alexa Fluor 488 phalloidin (Life Technologies). Cells were imaged using an Eclipse Ti-E (Nikon).

Data Analysis and Statistics. Immunoblot results were quantified using a Kodak Gel Logic 100 imaging system equipped with Molecular Imaging 5.X software (Carestream Health, New Haven, CT) to calculate Gaussian fit for each protein band. For graphical data presentation, error bars represent either ± range or ± S.E.M., as indicated in the figure legends (Figs. 1–7). Student's t test with unequal variance was used to compare the means of two data sets with one measurement variable, and the Kruskal–Wallis test was

used for one-way analysis of variance. A *P* value < 0.05 was considered significant.

Results

Identification and Mutation of Class-Distinctive Residues within Gα₁₂. Each Gα class is thought to signal to its downstream effectors via specialized contact surfaces that are ultimately determined by primary sequence. Therefore, we hypothesized that these effector-binding surfaces harbor unique, "class-distinctive" amino acids that confer specificity for downstream signaling partners. To identify G12/13 class-distinctive residues, we conducted a structural alignment of all four classes of mammalian G protein α-subunits: Gs, Gi, Gq, and G12/13 as described by Temple et al. (2010) and identified 19 class-distinctive residues in the G12/13 class. Of these residues, 16 were located either in Gα₁₂ alone or in both Gα₁₂ and Gα₁₃ and were selected for further study. Through ancestral reconstruction analyses, we determined that the "nonclass-distinctive" counterpart, represented by a residue invariant among the other three mammalian Gα classes, most frequently represents the ancestral amino acid value (Temple et al., 2010). We engineered substitutions within a myc-tagged, constitutively active variant (Q229L) of Gα₁₂, termed myc-Gα₁₂^QL, with each mutation converting a class-distinctive residue to its nonclass-distinctive form (Fig. 1A). Each mutant was engineered as a single substitution, with the exception of Q232E/Q234K in which two Gln residues were changed in the same construct, yielding a total of 15 Gα₁₂ variants. When expressed in HEK293 cells, nearly all class-distinctive mutants were detected at levels comparable to unaltered myc-Gα₁₂^QL (Fig. 1B). Endogenous Gα₁₂ migrated slightly faster on gels than the myc-tagged variants and was not detectable (Fig. 1B, vector) except when immunoblots were developed for relatively long times.

Class-Distinctive Gα₁₂ Mutants Selectively Uncoupled from SRE Activation and Hsp90 Binding. We examined the Gα₁₂ class-distinctive mutants for activation of SRE-mediated transcription, a Rho-dependent cell growth pathway that is responsive to Gα₁₂ and Gα₁₃ (Fromm et al., 1997; Bhattacharyya and Wedegaertner, 2000). As shown in Fig. 2A, most of these mutants displayed normal or moderately impaired ability to stimulate a SRE-luciferase reporter construct (>50% of control, nonmutated myc-Gα₁₂^QL); however, the mutant L201R and the double-mutant Q232E/Q234K showed severe impairment of SRE stimulation (<20% of control), whereas the mutant F237I showed near-complete loss of SRE activation that was comparable to a constitutively inactive mutant (G228A) of Gα₁₂ that is unable to release GDP (Miller et al., 1988). We further tested these SRE-uncoupled Gα₁₂ mutants for an additional readout in this signaling pathway, nuclear translocation of MRTF-A/megakaryoblastic leukemia 1. This trafficking is mediated by activated Gα₁₂ and Gα₁₃ and requires downstream Rho activation, which participates in mediating MRTF-A nuclear import and activity by decreasing the availability of the MRTF-A binding partner, G-actin (Evelyn et al., 2007; Medjkane et al., 2009). As shown in Fig. 2B, cells expressing EGFP-tagged MRTF-A and cotransfected with myc-Gα₁₂^QL showed a higher percentage of cells with exclusively nuclear EGFP-MRTF-A staining than cells cotransfected with the inactive (G228A) myc-Gα₁₂. Although the SRE-uncoupled mutants of myc-Gα₁₂^QL (L201R, Q232E/Q234K,

F237I) showed varied results in this assay, all exhibited a lower percentage of cells with nuclear EGFP-MRTF-A localization than the positive control myc-Gα₁₂^QL, suggesting the impaired ability of these mutants to signal to SRE involves a mechanism upstream of MRTF-A transport to the nucleus.

In parallel to the SRE activation studies shown in Fig. 2A, we examined whether mutation of class-distinctive residues in Gα₁₂ to their nonclass-distinctive forms disrupted interaction with specific effector proteins. Myc-tagged Gα₁₂^QL and its mutants were expressed in HEK293 cells and tested for the ability to bind GST fusions of p115RhoGEF, LARG, and Hsp90 (Fig. 3A). As shown in Fig. 3B, each of these proteins was able to precipitate myc-Gα₁₂^QL from cell extracts.
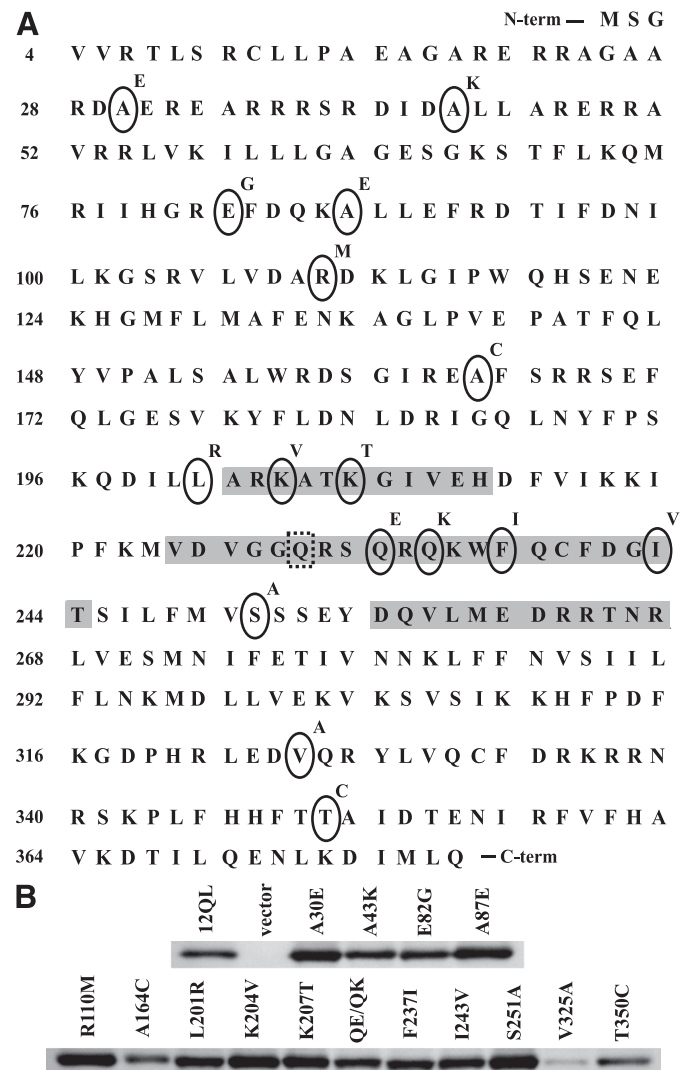

Fig. 1. Construction, expression, and solubilization of class-distinctive Gα₁₂ mutants. (A) Amino acid sequence of Gα₁₂ is shown. Each class-distinctive residue, indicated by an oval, was mutated to its nonclass-distinctive form (above right of ovals) in myc-tagged, constitutively active Gα₁₂. Shaded areas indicate the switch I, II, and III regions, and the dashed box indicates the site of the activating Q229L mutation. (B) The indicated mutant constructs were expressed in HEK293 cells, from which detergent-soluble extracts were subjected to immunoblot analysis as described in *Materials and Methods*. All mutants were single amino acid substitutions except the double-mutant Q232E/Q234K (*QE/QK*). Extracts from cells transfected with the Q229L variant of myc-tagged Gα₁₂ (*12QL*) and empty pcDNA3.1 (vector) were analyzed in parallel.
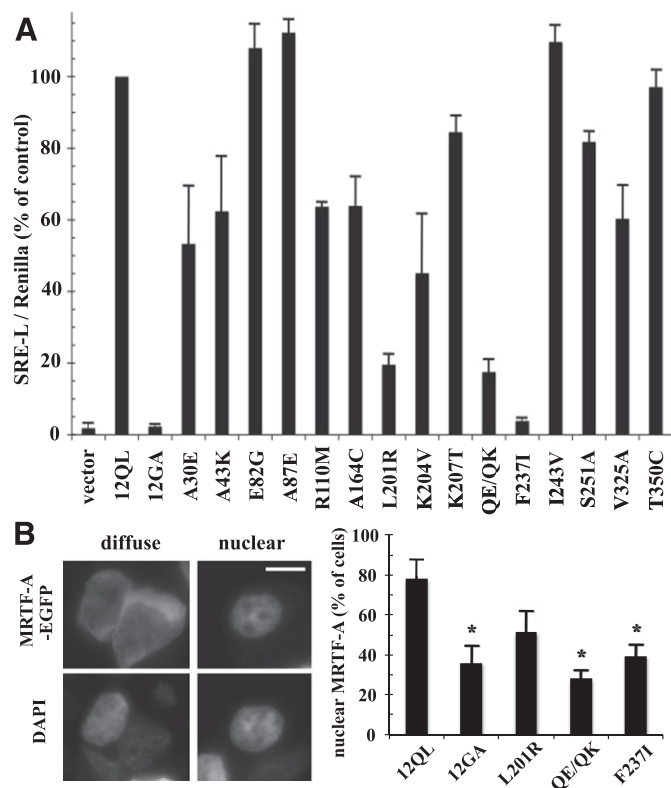
Fig. 2. Identification of class-distinctive mutants of Gα₁₂ impaired in SRE-mediated transcriptional activation. (A) HEK293 cells were transfected with the plasmids SRE-luciferase (0.2 μg) and pRL-TK (0.02 μg) plus 1 μg of plasmid encoding each indicated class-distinctive mutant of myc-Gα₁₂^{QL} (x-axis). Firefly luciferase activity values were normalized for *Renilla* luciferase activity values and presented as a percent of positive control myc-Gα₁₂^{QL} (*12QL*) within the same experiment. Empty pcDNA3.1 (vector) and Gα₁₂ harboring the inactivating G228A mutation (*12GA*) were examined as negative controls. Data presented are the mean ± range of two independent experiments per myc-Gα₁₂^{QL} variant, with three or more experiments performed for mutants that showed greater than 50% impairment of SRE stimulation. (B) HEK293 cells grown in six-well plates were cotransfected with 1.0 μg of EGFP-MRTF-A plasmid and 1.0 μg of each indicated Gα₁₂ construct. Cells (50 per transfection) were scored for either diffuse or exclusively nuclear localization of the EGFP signal, using 4′,6-diamidino-2-phenylindole (DAPI) costaining to define the boundaries of the nucleus. Examples are shown in the left panels (two cells exhibiting diffuse EGFP-MRTF-A staining) and right panels (single cell exhibiting nuclear staining of EGFP-MRTF-A). Scale bar is 10 μm. The column graph shows results compiled from three independent trials, presented as mean ± S.E.M. Significance of the difference in mutant values compared with positive control (*12QL*) was determined by Student's *t* test (*$P < 0.05$).

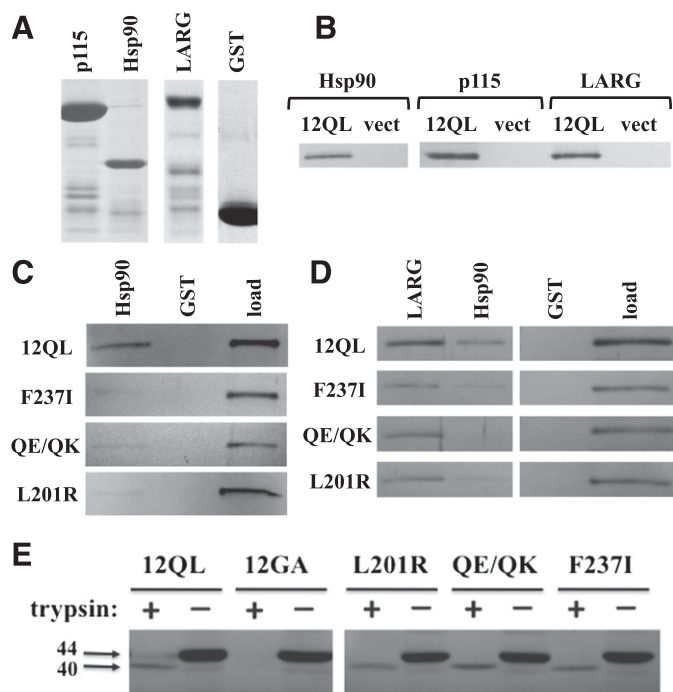**Fig. 3.** Effector binding and conformational activation of SRE-uncoupled class-distinctive Gα₁₂ mutants. (A) GST fusions of the N-terminal 252 amino acids of p115RhoGEF (*p115*), the C-terminal 107 residues of cytoplasmic *Hsp90*, and the region spanning Leu320 to Arg606 of *LARG* were analyzed by SDS-PAGE and Coomassie blue staining. Unmodified GST was analyzed in parallel. (B) Coprecipitation experiments using these GST fusion proteins were performed on detergent extracts from HEK293 cells expressing myc-tagged, constitutively active Gα₁₂ (12QL) or empty pcDNA3.1 (vect). (C) Coprecipitations of indicated Gα₁₂ mutants by immobilized Hsp90 are shown. For each panel, the left and center lanes harbor samples in which Sepharose-bound GST-Hsp90 or GST (indicated at top) were used to precipitate fractions from HEK293 extracts harboring myc-Gα₁₂^{QL} (*12QL*) or the mutants indicated at left. The right lane of each panel (load) harbors 5% of the HEK293 extract set aside before coprecipitation, and band intensities at ~44 kDa were quantified and used to normalize the coprecipitated bands for Gα₁₂ variants indicated here, as well as others (Table 1). A representative of three independent experiments is shown. (D) Coprecipitation of myc-Gα₁₂^{QL} and its indicated mutants by multiple effectors are shown. The indicated GST fusions of LARG and Hsp90, plus GST with no adduct (*GST*) are indicated, along with the load for each sample. Data shown are a representative of three independent experiments. (E) Trypsin protection assays were performed on the indicated class-distinctive mutants, plus constitutively activated (*12QL*) and inactivated (*12GA*) myc-Gα₁₂. HEK293 cells grown in 10-cm plates were transfected with 10 μg of plasmid DNA, and after 40 hours, cell lysates were subjected to tryptic proteolysis as described in *Materials and Methods*. Molecular weights are indicated at left in kilodaltons. Results shown are one representative of three independent experiments.

Among the class-distinctive mutants, L201R, F237I, and Q232E/Q234K were most severely impaired in binding Hsp90, with a precipitate-to-load ratio between 0 and 20% of the value for myc-Gα₁₂^{QL} (Fig. 3C; Table 1). This indicated that the subset of Gα₁₂ class-distinctive residues most indispensable for stimulating SRE-mediated transcription were also the most important in Gα₁₂–Hsp90 interaction. These mutations that attenuated SRE signaling and Hsp90 binding did not globally affect Gα₁₂ interaction with downstream targets, as all three mutants bound strongly to LARG and p115RhoGEF (Fig. 3D; Table 1). Furthermore, these mutations did not disrupt Gα₁₂ structural conformation. As shown in Fig. 3E, the mutants L201R, F237I, and Q232E/Q234K yielded a trypsin-protected 40-kDa fragment comparable to the fragment generated from nonmutated myc-Gα₁₂^{QL}, whereas the inactive G228A variant of

myc-Gα₁₂ was fully digested. Therefore, it appears these Gα₁₂ mutants retain fundamental properties of guanine nucleotide binding, and their impairment in SRE stimulation and Hsp90 binding appears not to be caused by failed conformational activation or other, nonspecific disruptions of protein folding or effector binding.

Phylogenetic Substitutions of Class-Distinctive Gα₁₂ Residues Have Differential Effects on SRE Signaling. In addition to comparing the different mammalian Gα classes to identify residues that confer signaling specificity, we determined the phylogenetic timeline of G12/13 class-distinctive residues by comparing divergent sequences from sea sponge, roundworm, fruit fly, sea urchin, and mouse or human (Temple et al., 2010). Evolutionary emergence of the

TABLE 1
Coprecipitation of Gα₁₂ class-distinctive mutants by downstream effectors

For each class-distinctive mutant of myc-Gα₁₂^{QL} (left column), precipitation by each GST-fused effector protein (top row) and starting material (i.e., load) were quantified as described in *Materials and Methods* to determine a precipitate:load ratio. Categories are as follows: ++++, ratio >70% of positive control myc-Gα₁₂^{QL}; +++, 40–70% of control; ++, 20–40% of control; +, 0–20% of control; −, no detectable coprecipitation. Each sample is the result of two trials, except for samples scoring ++, +, or −, which were analyzed in at least three trials.

	p115	LARG	Hsp90
A30E	++++	++++	++/+++
A43K	+++	+++	+++
E82G	++++	++++	++++
A87E	++++	++++	++++
R110M	++++	++++	++
A164C	++/+++	+++	++++
L201R	++++	+++	−/+
K204V	+++	+++	++/+++
K207T	++++	++++	++
QE/QK	+++	++++	−/+
F237I	++/++++^{a}	++++	+
I243V	++/+++	+++	++++
S251A	++	++++	+++
V325A	+++	+++/++++	+++
T350C	++	++	++

^{a}Variation spanning more than two categories.

Leu residue immediately upstream of the switch I region (Leu201 in Gα₁₂; Leu198 in Gα₁₃) was relatively recent for the G12/13 class because a His residue occupies this position in the sea urchin and *Drosophila* homologs, and the *Caenorhabditis elegans* and sea sponge G12/13 proteins harbor other residues (Fig. 4A). In contrast, Phe237 in the switch II region of Gα₁₂ is highly conserved in G12/13 proteins of all the taxa examined (Fig. 4A) except *Drosophila*, in which Thr occupies this position. To assess the structural and functional consequences of these evolutionary changes within the G12/13 class, we mutated Leu201 and Phe237 in myc-Gα₁₂^{QL} to the corresponding *Drosophila* residues His and Thr, respectively. The L201H mutant (i.e., mammal → fly) exhibited normal SRE activation and binding to Hsp90, in sharp contrast to L201R (i.e., class-distinctive → nonclass-distinctive) that caused impairment of both functions (Fig. 4, B and C). Surprisingly, the F237T mutant (mammal → fly) in myc-Gα₁₂^{QL} showed near-complete loss of SRE stimulation (Fig. 4B), phenocopying the Phe237 mutation to Ile (class-distinctive → nonclass-distinctive), and both F237I and F237T mutants were markedly impaired in Hsp90 binding (Fig. 4C). For all variants of residues Leu201 and Phe237 that we engineered, binding of Gα₁₂ to LARG was unperturbed or slightly diminished (Fig. 4C). In some experiments, protein levels of mutants L201R and F237I were lower than the positive control myc-Gα₁₂^{QL}; therefore, to ascertain that impaired SRE signaling was not due merely to lowered expression of these mutants, we examined a series of cell samples transfected with decreasing amounts of myc-Gα₁₂^{QL} plasmid (Fig. 4B). Mutants F237I and L201R showed impaired SRE activation compared with myc-Gα₁₂^{QL} expressed at similar levels. From these data, we conclude that Leu201 and Phe237 in mammalian Gα₁₂ were critical components of its evolved ability to stimulate SRE and bind Hsp90, but the corresponding residues in the *Drosophila* G12/13 homolog Concertina represent different stages of this process. The His residue upstream of the switch I region in Concertina is effectively a G12/13 class-distinctive residue
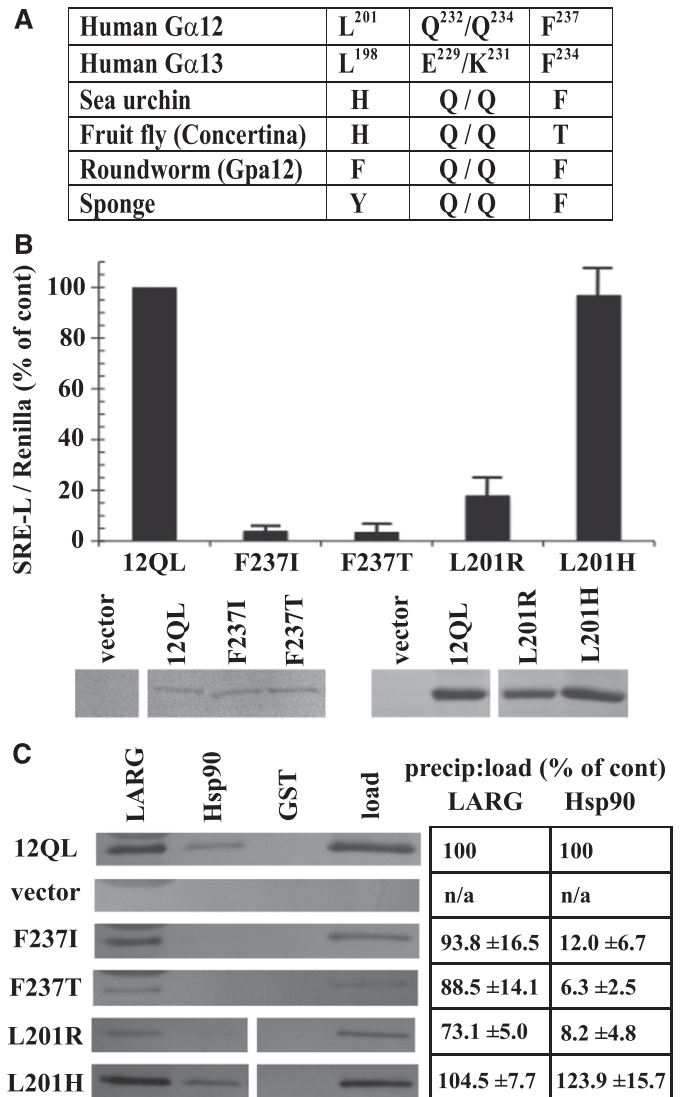
Human Gα12	L^{201}	Q^{232}/Q^{234}	F^{237}
Human Gα13	L^{198}	E^{229}/K^{231}	F^{234}
Sea urchin	H	Q / Q	F
Fruit fly (Concertina)	H	Q / Q	T
Roundworm (Gpa12)	F	Q / Q	F
Sponge	Y	Q / Q	F

	precip:load (% of cont)	
	LARG	Hsp90
12QL	100	100
vector	n/a	n/a
F237I	93.8 ±16.5	12.0 ±6.7
F237T	88.5 ±14.1	6.3 ±2.5
L201R	73.1 ±5.0	8.2 ±4.8
L201H	104.5 ±7.7	123.9 ±15.7

Fig. 4. Ancestral and Concertina-specific substitutions of Gα₁₂ residues involved in SRE activation and Hsp90 binding. (A) An evolutionary profile of selected class-distinctive G12/13 residues is shown, with position in the primary amino acid sequence shown in superscript for Gα₁₂ and Gα₁₃ (Temple et al., 2010). (B) The indicated substitutions in myc-Gα₁₂^{QL} (x-axis) were examined for SRE-luciferase activation as described in *Materials and Methods*, and results are presented as a percent of positive control myc-Gα₁₂^{QL} (*12QL*). Panels beneath this graph show expression levels of the indicated mutants, matched with one of several different samples of myc-Gα₁₂^{QL}, as determined by immunoblot analysis of HEK293 cell lysates using anti-Gα₁₂ antibody. (C) Effects of the indicated substitutions within Gα₁₂ on coprecipitation by immobilized LARG and Hsp90 are shown, with lysates from cells transfected with myc-Gα₁₂^{QL} and empty vector analyzed in parallel. Panel at left shows blot images representative of three independent experiments, and panel at right shows precipitate-to-load ratios as a percent of the same ratio determined for myc-Gα₁₂^{QL} (set at 100%). Quantitative data are presented as mean ± S.E.M.

(i.e., facilitated the same signaling properties as Leu201 in Gα₁₂) and therefore might be an intermediate to fixation of the Leu residue in mammalian G12/13 proteins. On the other hand, the Thr residue in the switch II region of Concertina fails to act as a G12/13 class-distinctive residue; its introduction to Gα₁₂ disrupted both SRE-mediated signaling and Hsp90 binding. It remains to be determined whether this Thr residue confers a unique signaling property in Concertina

despite the conservation of Phe at this position in the G12/13 class from sea sponge to humans. To our knowledge, these results provide the first instance of a signaling function being disrupted in a mammalian G12/13 protein by substitution of corresponding sequence from an evolutionary homolog in the same class.

Structural Determinants of Hsp90 Interaction Are Selectively Required for Gα_{12} in G12/13-Mediated SRE Activation. Gα_{13}, like Gα_{12}, is a potent stimulator of SRE-mediated transcriptional activation (Fromm et al., 1997), and activated mutants of both Gα_{12} and Gα_{13} are blocked in SRE activation by the *Clostridium botulinum* C3 exoenzyme, a specific inhibitor of Rho activity (Shi et al., 2000). To assess the requirement for Hsp90 function in Gα_{12} and Gα_{13} signaling, we used a constitutively active (Q226L) variant of Gα_{13} along with constitutively active Gα_{12} and examined effects of the Hsp90 inhibitor geldanamycin on SRE activation. Hydrolysis of ATP is critical for Hsp90 in forming a "clamped" complex with client proteins, and geldanamycin disrupts this biologic function of Hsp90 by competing for ATP binding to the N-terminal domain (Peterson and Blagg, 2009). We found geldanamycin to partially block Gα_{12}-mediated activation of SRE-luciferase in HEK293 cells, whereas this compound showed significantly lower efficacy in blocking Gα_{13} stimulation of this reporter (Fig. 5A). This selectivity of geldanamycin on Gα_{12} signaling within the G12/13 class agreed with previous findings in NIH3T3 fibroblasts (Vaiskunaite et al., 2001). In addition, we tested the ability of Gα_{12} and Gα_{13} to stimulate SRE-luciferase in HEK293 cells cotransfected with siRNA targeting human Hsp90-α. These experiments yielded results similar to the effects of geldanamycin; this RNA interference caused significantly greater downregulation of Gα_{12}-mediated SRE activation in comparison with the Gα_{13}-driven response (Fig. 5A). To determine whether the SRE-uncoupled mutants define a mechanism specific to Gα_{12} within the G12/13 family, we engineered constitutively active Gα_{13} to harbor substitutions of Leu198 and Phe234 to their nonclass-distinctive forms (mutants L198R and F234I) and their Concertina-specific forms (mutants L198H and F234T). In striking contrast to Gα_{12}, these substitutions in Gα_{13} caused no disruption in SRE signaling (Fig. 5B). We also examined the role of Gα_{13} residues that correspond to the class-distinctive Gln232/Gln234 pair found in Gα_{12}. As described already herein (Figs. 2 and 3), the Q232E/Q234K mutant converts Gln residues within the Gα_{12} switch II region to their nonclass-distinctive forms, disrupting SRE stimulation and Hsp90 binding. Paradoxically, these nonclass-distinctive Glu and Lys residues are present in Gα_{13}, despite conservation of the Gln/Gln pair in the G12/13 class for all nonmammalian taxa examined (Fig. 4A). We hypothesized that "reversion" from Gln/Gln to the ancestral Glu/Lys was necessary for Gα_{13} to evolve its distinct mechanism of growth signaling, and therefore we mutated Glu229 and Lys231 in Gα_{13} to a pair of Gln residues and tested this E229Q/K231Q mutant in SRE-luciferase assays. Surprisingly, these substitutions caused no disruption of SRE activation triggered by constitutively active Gα_{13} (Fig. 5B), suggesting that Glu229 and Lys231 of Gα_{13} are uninvolved in its stimulation of SRE-mediated transcription, whereas Gln residues at these positions in Gα_{12} are critical for its mechanism of activating the same response. A structural comparison of Gα_{12} to Gα_{13} in the switch II region reveals

similarities and differences in backbone and side-chain atoms at the Q232E/Q234K positions (Fig. 5C). In Gα_{12}, the Q232E substitution alters only the charge of the side-chain, whereas the Q234K substitution changes both size and charge. Taken as a whole, these findings suggest that the effector proteins stimulated by Gα_{12} and Gα_{13} in the pathway(s) leading to SRE-mediated transcription are not identical and that interaction with functional Hsp90 is a specific requirement of Gα_{12} in this signaling response.

Class-Distinctive Mutants of Gα_{12} Uncouple SRE Activation from Rho-Mediated Signaling. Our results, shown in Fig. 4, revealed a single amino acid substitution (F237T; mammal → fly) that uncoupled Gα_{12} from SRE activation, and this finding compelled us to examine whether the *Drosophila* Gα_{12} homolog Concertina could stimulate the SRE pathway when expressed in mammalian cells. Concertina is required for cell shape changes and migration during gastrulation (Parks and Wieschaus, 1991), but its growth signaling properties are not known. Because Concertina-specific antibodies were not available, we subcloned both wild-type and constitutively active Concertina (both Q303L and R277C variants) into the mammalian cell expression vector pLL5.5 (Uetrecht and Bear, 2009) harboring an IRES to allow translation from a bicistronic mRNA, along with green fluorescent protein (GFP). Neither wild-type nor constitutively active Concertina (Q303L or R277C) stimulated SRE-luciferase when expressed ectopically in HEK293 cells, despite the expression of GFP (Fig. 6A). We were not able to obtain a definitive result in experiments testing ability of the Q303L variant of Concertina to trigger a cytoskeletal response in HEK293 cells (data not shown); however, this Q303L variant was functional in its normal cellular context as an activator of contractility in S2 cells (Fig. 6, B and C), as was the R277C variant (data not shown). As a result of the acute disruption of Gα_{12}-mediated SRE signaling observed when Phe237 was converted to the Concertina-specific Thr, we engineered the converse mutant by replacing Thr311 of Concertina with the Gα_{12}-specific Phe residue. However, this T311F substitution did not confer on Concertina the ability to activate SRE-mediated transcription in HEK293 cells (Fig. 6A).

Of the class-distinctive Gα_{12} residues we identified as critical for SRE activation, only the switch II region Gln/Gln pair is conserved between Gα_{12} and Concertina. To determine whether these Gln residues are important in Concertina-driven cytoskeletal rearrangements, which is a signaling pathway known to use the RhoGEF-Rho axis (Barrett et al., 1997), we tested a Q306E/Q308K mutant of constitutively active Concertina (Q303L) for the ability to stimulate S2 cell contraction. This Concertina mutant showed no loss of efficacy in triggering contractility of S2 cells (Fig. 6, B and C), suggesting that these Gln residues are not involved in the Gα-driven mechanism that mediates these Rho-dependent cytoskeletal changes. We also directly examined the SRE-uncoupled Gα_{12} mutants (L201R, F237I, and Q232E/Q234K) for Rho activation, by using RBD assays to selectively precipitate GTP-bound RhoA from HEK293 cell lysates. As shown in Fig. 6D, the F237I and L201R mutants showed activation of Rho comparable to positive control myc-Gα_{12}^{QL}. The Q232E/Q234K mutant of myc-Gα_{12}^{QL} triggered a low, although significant, activation of Rho in comparison with inactive, GDP-bound myc-Gα_{12}, despite the robust cytoskeletal response triggered in S2 cells by Concertina harboring the same substitutions.
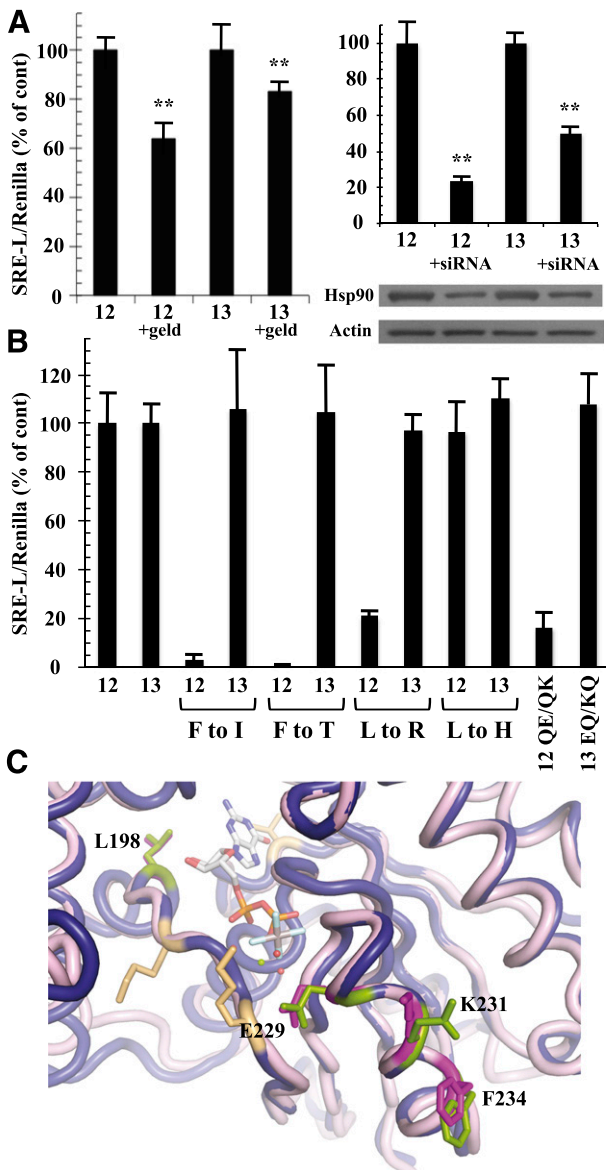
Fig. 5. Differential effects of Hsp90 inhibition and SRE-uncoupling mutations in Gα₁₂ and Gα₁₃. (A) Effects of geldanamycin (left graph) and Hsp90-specific siRNA (right graph) on Gα₁₂- and Gα₁₃-mediated SRE activation are shown. HEK293 cells grown in 12-well plates were transfected with 0.2 μg of SRE-luciferase and 0.02 μg of pRL-TK, plus 1 μg of a constitutively active variant of either Gα₁₂ (12) or Gα₁₃ (13). For the left graph, cells were serum-starved for 24 hours, and then 1 μg/ml geldanamycin (geld) was added for 6 hours. For the right graph, siRNA specific to cytoplasmic Hsp90-α was cotransfected with the above plasmids as described in *Materials and Methods*. Luminometry assays were performed as described in Fig. 2, and each G12/13 control sample (geldanamycin absent, or siRNA absent) was set at 100%. For siRNA experiments, cell lysates were subjected to immunoblot analysis, using antibodies specific to Hsp90-α (Santa Cruz Biotechnology) and actin (clone C4; Millipore), and representative blots are shown. Results presented in each graph are the mean of three or more independent experiments, with error bars representing ± S.E.M. Effects of geldanamycin (left graph) and siRNA (right graph) were analyzed by one-way analysis of variance for significant difference in disruption of the Gα₁₂ response compared with disruption of the Gα₁₃ response (**P < 0.001). (B) HEK293 cells were transfected with SRE-luciferase and pRL-TK as described above plus 1 μg of each Gα plasmid. All constructs encoded the constitutively active form of the Gα protein (12 or 13), and substitutions of class-distinctive residues are indicated below the *x*-axis (e.g., *F to I*). Additional mutants were tested: *QE/QK*, Q232E/Q234K substitutions in constitutively active Gα₁₂; *EQ/KQ*, E229Q/K231Q substitutions in constitutively active Gα₁₃. Data are presented as mean ± range and are the result of three or more independent experiments per construct. (C) Rendering of Gα₁₂ (PDB ID 1ZCA; Kreutz

Gα₁₂ Switch Regions and C Terminus Harbor Independent Determinants of SRE Activation. Because Concertina failed to stimulate SRE-mediated transcription in HEK293 cells, we used this *Drosophila* Gα₁₂ homolog as a "blank canvas" in these mammalian cells for identifying regions of Gα₁₂ that mediate SRE activation. We engineered a set of Gα₁₂/Concertina chimeras, designated numbers 1–6, in which a domain encompassing the three switch regions and the flanking N- and C-terminal domains were interchanged in all possible combinations (Fig. 7A). Each chimera was engineered to harbor an activating Gln-to-Leu mutation within the switch II region and was subcloned into the IRES vector pLL-5.5 to allow normalization of expression through GFP immunoblotting (Uetrecht and Bear, 2009). Strikingly, the only construct that stimulated SRE signaling was chimera 4, which harbors the N-terminal 275 residues of Concertina and an additional 178 residues comprising the switch regions and C terminus of Gα₁₂ (Fig. 7B). Whereas this chimera showed robust SRE activation equal to or greater than myc-Gα₁₂^QL, the other chimeras exhibited no SRE stimulation, with readings comparable to mutationally activated Concertina or the IRES vector expressing GFP only (Fig. 7B). GFP levels in cell lysates were similar, suggesting that the bicistronic mRNAs encoding all six chimeras were comparable in levels and translation rate (Fig. 7B). These results indicated the switch regions and C-terminal domain of Gα₁₂ harbor determinants that are independently required for SRE activation in HEK293 cells because replacement of either domain with Concertina sequence abrogated this response. To define determinants within the Gα₁₂ C terminus critical for this signaling function, we aligned the Gα₁₂ and Concertina C-terminal domains and found two regions of close homology, separated by a divergent region spanning Lys304 to Phe345 in Gα₁₂ and Cys379 to Tyr423 in Concertina (Fig. 7A). To determine whether this region harbors Gα₁₂-specific determinants of SRE activation, we engineered a "sub-chimera" (designated chimera 4-sub) in which this Gα₁₂ region in chimera 4 was replaced by Concertina sequence. Because N-terminal epitope-tagging of Concertina did not disrupt its ability to stimulate S2 cell contraction (Fig. 6, B and C), we engineered an N-terminal myc tag in chimeras 4 and 4-sub and similarly tagged the other chimeras that harbored the Concertina N-terminal domain (chimeras 3 and 5). As shown in Fig. 7C, chimera 4-sub displayed near-complete loss of SRE signaling, even though immunoblots showed similar expression levels to chimera 4. Myc-tagged chimeras 3, 4, and 5 generated essentially the same SRE-luciferase readouts as their untagged forms (data not shown). We also generated a variant of myc-Gα₁₂^QL, designated Δ45, harboring a substitution that introduced the same C-terminal 45-residue Concertina sequence found in chimera 4-sub, and as predicted, this mutation caused a complete loss of SRE activation (Fig. 7C). The corresponding Δ45 mutant of Gα₁₃^QL, in which its region spanning Gln301 to Tyr343 was replaced by the

et al., 2006) is shown in blue cartoon and Gα₁₃ (PDB ID 3AB3; Hajicek et al., 2011) in light pink cartoon with the bound nucleotide displayed as sticks and colored by atom type with carbons in white. For Gα₁₃, side chains of Leu198, Glu229, Lys231, and Phe234 are displayed as magenta sticks and numbered. Corresponding Gα₁₂ side chains of Leu201, Gln232, Gln234, and Phe237 are shown as green sticks and are not numbered in this diagram. Figure was rendered in The PyMOL Molecular Graphics System, Version 1.5.0.1 Schrödinger, LLC.
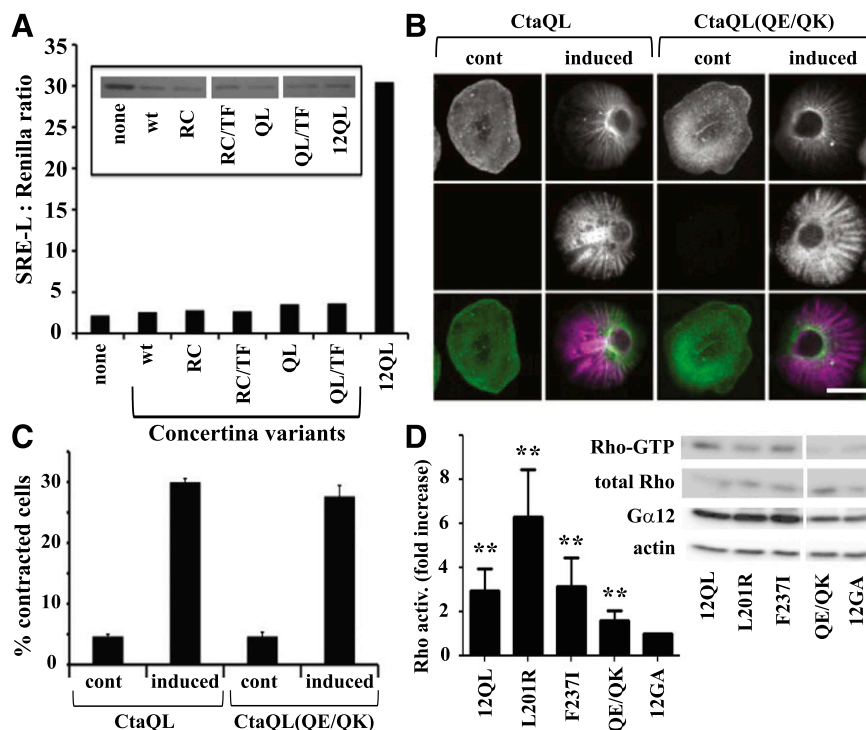
Fig. 6. Differential effects of Gα₁₂ and Concertina on SRE-mediated transcription and cytoskeletal rearrangements. (A) Effect of Concertina variants on SRE-mediated transcriptional activation. HEK293 cells were transfected with a GFP-encoding IRES vector harboring myc-Gα₁₂^QL (*12QL*), no additional coding sequence (*none*), or Concertina variants with the following designations: *wt*, wild-type; *RC*, R277C; *QL*, Q303L; *TF*, T311F. For each sample, luciferase assays were performed (graph) and GFP levels were determined by immunoblot analysis (inset) to allow indirect measure of expression of Concertina variants. Data shown are a representative of three independent experiments. (B) Effect of Concertina and its Q306E/Q308K variant on cell contraction. S2 cells expressing inducible myc-tagged, constitutively active Concertina (*CtaQL*) or the same protein harboring Q306E/Q308K substitutions (*QE/QK*) were induced with 50 μM copper sulfate and 24 hours later scored for contractility as described in *Materials and Methods*. Cells were stained with phalloidin (top row) and anti-myc antibody (middle row), and images were merged (bottom row). Scale bar is 10 μm, and images are from a representative of three independent experiments. (C) Compiled quantitative data from experiments described in (B) are shown, with bars indicating S.E.M. (D) HEK293 cells were assayed for basal RhoA activity 36–42 hours after transfection with constitutively active (*12QL*) or inactive (*12GA*) myc-tagged Gα₁₂, or the indicated mutants of myc-Gα₁₂^QL. Blots were developed with SuperSignal West Pico chemiluminescent substrate (Pierce, Rockford, IL) and Kodak Biomax film, and representative blots of active RhoA (*Rho-GTP*) precipitated by GST-RBD versus total RhoA in cell lysates are shown, along with blots of Gα₁₂ and actin in the same experiment. RhoA activity is the ratio of active RhoA to total RhoA signal, with densitometry (NIH ImageJ software) used to quantify results from seven independent experiments. Results are graphed as the -fold increase over cells expressing inactive, GDP-bound Gα₁₂ (*12GA*). Graphical data represent mean ± S.E.M.; **$P < 0.001$ as calculated through analysis of variance using the Kruskal–Wallis test.

aforementioned Concertina sequence, exhibited robust SRE stimulation (Fig. 7C). These findings bolster our results shown in Fig. 5, suggesting that Gα₁₂ and Gα₁₃ use different structural features and effector binding events in stimulating this cell proliferative pathway. Taken as a whole, our results define specific residues in the switch regions, as well as a region near the C terminus, that differ between Gα₁₂ and its *Drosophila* homolog and are required for SRE signaling by Gα₁₂, but not Gα₁₃.

Discussion

To illuminate the structural features of Gα₁₂ and Gα₁₃ that mediate their signaling functions, a useful approach has been to test mutants for disruption of cellular responses or binding to downstream targets (Jones and Gutkind, 1998; Adarichev et al., 2003; Nakamura et al., 2004; Vazquez-Prado et al., 2004; Grabocka and Wedegaertner, 2005). Such studies have revealed Gα₁₂ determinants of binding to effectors that include RhoGEFs, protein phosphatase-2A, and polycystin-1 (Meigs et al., 2005; Zhu et al., 2007; Yu et al., 2011). Our current study was guided by a method that identified "class-distinctive"

residues within each Gα protein and deduced the ancestral, "nonclass-distinctive" residue at each position (Temple et al., 2010). We engineered a panel of Gα₁₂ mutants by converting each class-distinctive residue to its nonclass-distinctive counterpart; these substitutions were intended to render features of Gα₁₂ as ancestral-like conformations that might lack ability to engage specific targets. These mutants revealed Gα₁₂ residues required for binding to Hsp90 but not RhoGEFs: Leu201 just upstream of the switch I region and Phe237 and Gln232/Gln234 within the switch II region. Unexpectedly, these mutations matched the subset of class-distinctive substitutions we identified as disruptive to Gα₁₂ stimulation of SRE-mediated transcription. The effects of geldanamycin, which inhibits ATP binding to the Hsp90 homodimer and would be predicted to disrupt its functional interaction with client proteins that include Gα₁₂, suggest a relationship between Gα₁₂-Hsp90 interaction and SRE activation, and this hypothesis is further supported by our results after siRNA-mediated targeting of Hsp90 expression (Fig. 5). However, the incomplete effect of geldanamycin on Gα₁₂-stimulated SRE signaling leaves open the possibility that the aforementioned class-distinctive mutations disrupt SRE signaling by hindering Gα₁₂
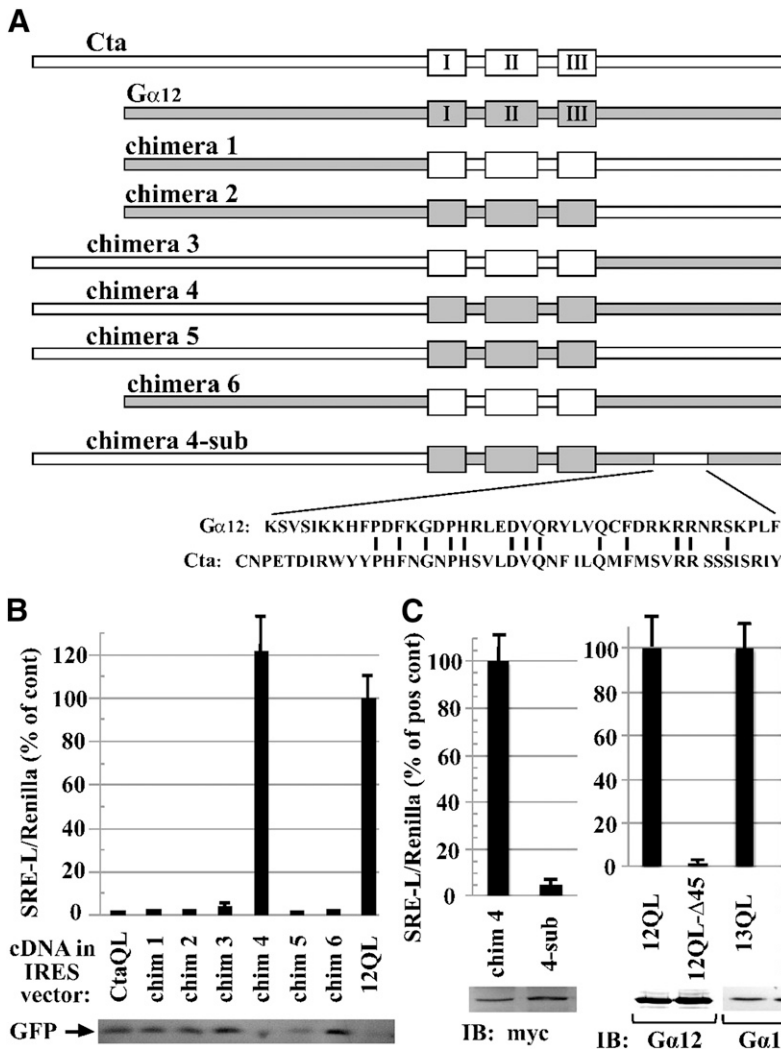
Fig. 7. Identification of additional determinants of SRE activation in Gα_{12}. (A) Schematic of Gα_{12}/Concertina chimeras is shown. Chimeras were engineered as described in *Materials and Methods*, with the switch regions demarcated by the N-terminal boundary of the switch I region (Cys276 of Concertina, Ala202 of Gα_{12}) and the C-terminal boundary of the switch III region (Arg342 of Concertina, Arg267 of Gα_{12}). An activating Gln-to-Leu mutation was engineered in the switch II region of each construct. For chimera 4-sub, the indicated 45-residue Concertina region was introduced to chimera 4 in place of the indicated 42-residue Gα_{12} region. (B) Stimulation of SRE-mediated transcription in HEK293 cells (see *Materials and Methods*) by Gα_{12}/Concertina chimeras 1–6 is shown. SRE activation is displayed as percent of the positive control myc-Gα_{12}^{QL} (*12QL*) in the same experiment. Values are mean $\pm$ range for three or more independent trials per chimera, with only the mean displayed for samples with values $\leq$3% of positive control. Immunoblot levels of GFP, coexpressed in the IRES vector harboring each chimera, are shown (lower panel). (C) Effects of C-terminal Concertina substitutions within chimera 4 and G12/13 proteins are shown. N-terminally myc-tagged chimera 4 and chimera 4-sub were tested for SRE activation, and mean $\pm$ range is shown for three independent experiments. Lysates were examined by immunoblot (IB) analysis using anti-myc antibody; results from a representative experiment are shown. SRE activation assays for mutants harboring the aforementioned 45-residue Concertina region at the C terminus of myc-Gα_{12}^{QL} (12QL-$\varDelta$45) and Gα_{13}^{QL} (13QL-$\varDelta$45) are presented in comparison with positive controls myc-Gα_{12}^{QL} and Gα_{13}^{QL}, respectively, and results are shown as mean $\pm$ range for three independent experiments. Comparative expression levels of the two Gα_{12} constructs, and the two Gα_{13} constructs, were determined by immunoblot analysis using anti-Gα_{12} (Santa Cruz Biotechnology) and anti-Gα_{13} (EMD Millipore) antibodies, and images from a representative experiment are shown.

interaction with other, unexamined binding partners in addition to Hsp90.

Gα_{12} signaling to SRE requires activation of Rho (Fromm et al., 1997). Because the SRE-uncoupled Gα_{12} mutants exhibited normal binding to RhoGEFs, as well as robust Rho activation for mutants L201R and F237I, these class-distinctive Gα_{12} residues may mediate engagement of an effector pathway(s) required in addition to the canonical RhoGEF-Rho pathway for SRE activation. Results for the Q232E/Q234K mutant of Gα_{12} were less clear; these substitutions disrupted SRE activation and also diminished Rho activation, even though RhoGEF binding remained intact. It is possible this mutation disrupts SRE signaling by partially uncoupling Gα_{12} from the RhoGEF-Rho signaling pathway. However, our finding that Concertina harboring the same mutation triggered normal Rho-mediated contractility in S2 cells (Fig. 6) suggests that this conserved Gln/Gln pair is not required for the ancient G12/13-RhoGEF-Rho axis that mediates cell shape changes in organisms such as *Drosophila* and *C. elegans* (Barrett et al., 1997; Yau et al., 2003). Our overall results suggest the L201R and F237I mutants are more decisive than the Q232E/Q234K mutant in selectively uncoupling Gα_{12} from Hsp90 without perturbing Gα_{12}-RhoGEF interaction. It is possible this Gln/Gln pair plays

a Gα_{12}-specific role in mediating Gα binding to a target protein (e.g., Hsp90) that must be engaged for RhoGEF-Rho signaling to commence. The *Drosophila* Gα_{12} homolog Concertina may lack this requirement, as its Q306E/Q308K mutant was unimpeded in triggering cytoskeletal rearrangements. Taken as a whole, our results suggest the class-distinctive residues essential for Gα_{12}-specific SRE activation either mediate a Rho-independent signaling pathway or participate in an effector binding event that facilitates coupling of Gα_{12} to the RhoGEF-Rho pathway.

Both Gα_{12} and Gα_{13} stimulate SRE-mediated transcription via mechanisms that are sensitive to Rho inhibition (Fromm et al., 1997; Bhattacharyya and Wedegaertner, 2000; Shi et al., 2000). However, Hsp90 perturbation preferentially hindered SRE activation by Gα_{12} in comparison with Gα_{13} (Fig. 5), suggesting that nonredundant signaling mechanisms evolved within the G12/13 class. Geldanamycin inhibits thrombin-mediated signaling through protease-activated receptor 1 in mouse neuroblasts but fails to inhibit LPA-mediated signaling (Pai and Cunningham, 2002), and because the thrombin receptor preferentially couples to Gα_{12} whereas LPA signaling uses Gα_{13} (Yamaguchi et al., 2003), this finding implicates Hsp90 in a Gα_{12}-specific role. Furthermore, our mutations of residues Leu201 and Phe237 disrupted Gα_{12} but

not Gα_{13} in stimulating SRE-mediated transcription, despite conservation of these amino acids in both proteins. Another apparent Gα_{12} determinant of SRE activation, the Gln232/ Gln234 pair, is conserved throughout taxa harboring the G12/ 13 class, whereas the Gs, Gi, and Gq classes use Glu/Lys at these positions. Therefore, it is intriguing that Gα_{13} "reverted" to the ancestral Glu/Lys pair during its evolution and that the Gln/Gln pair is critical for Gα_{12} in SRE activation, whereas Gα_{13} utilizes a signaling mechanism unaffected by Glu/Lys mutation to Gln/Gln. The functional significance of this Glu/Lys motif in Gα_{13} remains to be determined. Substitution of this Glu residue in Gα_{13} (Glu229) for a positively charged residue disrupted its RhoGEF binding, SRE activation, and recruitment of p115RhoGEF to the plasma membrane. Conversely, mutation of Glu229 to Ala did not disrupt RhoGEF binding by Gα_{13}, and effects on SRE signaling were not reported (Grabocka and Wedegaertner, 2005). Disruption of SRE signaling by charge reversal at this site may be due solely to interference with RhoGEF engagement, whereas E229Q substitution in our study allowed Gα_{13} to retain SRE activation and presumably functional RhoGEF binding.

Because Gα_{12} and Gα_{13} both stimulate SRE-mediated transcription, albeit through nonredundant mechanisms, the inability of the closely related Concertina to activate this pathway in HEK293 cells was surprising. It is possible that requisite downstream effector proteins in mammalian cells are not engaged by Concertina or that this fly protein fails to fold properly in these cells. However, our data from Gα_{12}/ Concertina chimeras (Fig. 7) demonstrate that the N-terminal 275 amino acids, as well as a 45-residue C-terminal region of Concertina, can fold correctly and facilitate robust Gα_{12}- or Gα_{13}-mediated signaling in HEK293 cells. These results suggest that key growth-signaling properties, including mechanisms potentially involved in oncogenic transformation, evolved in the lineage that yielded mammalian G12/13 proteins after divergence from Concertina. Moreover, because Concertina activates cytoskeletal rearrangements in *Drosophila* through a RhoGEF (DRhoGEF2) homologous to the G12/13-coupled mammalian RhoGEFs (Barrett et al., 1997), the striking difference in Gα_{12} and Concertina signaling to SRE in HEK293 cells bolsters the hypothesis that Gα_{12} stimulation of this response requires additional effector(s) in these cells besides the canonical RhoGEF-Rho axis. These findings compelled us to interchange residues between Gα_{12} and Concertina, revealing F237T mutation in Gα_{12} as disruptive to SRE activation in HEK293 cells, whereas replacement of the Gα_{12} residue Leu201 with the Concertina residue His had no apparent effect. These results suggest Concertina harbors some, not all, of the structural features necessary for SRE activation in mammalian cells and that such characteristics were partially in place in a common ancestor of Concertina and the mammalian G12/13 proteins. Furthermore, Concertina provided a uniquely useful "foil" for Gα_{12} in our study, due to its ~55% identical amino acid sequence and shared signaling properties in regulating Rho-mediated cytoskeletal rearrangements. Our experiments utilizing Gα_{12}/Concertina chimeras revealed both the domain encompassing the switch regions and a span near the Gα_{12} C terminus as harboring independent determinants of SRE activation. Furthermore, our studies using a corresponding Gα_{13}/Concertina chimera suggested that the same C-terminal

span in Gα_{13} is not involved in its signaling toward SRE activation. Future comparison of G12/13 proteins with these and other chimeras, in assays of effector binding and cellular signaling readouts, may reveal structural features and mechanisms used by Gα_{12} and Gα_{13} to activate proliferation, migration, and other responses.

A question that arises from our findings is: what advantage was gained by Gα_{12} and Gα_{13} evolving different mechanisms for stimulating SRE-mediated transcription? In considering this question, it is noteworthy that similar examples have been reported in the G12/13 class. Both Gα_{12} and Gα_{13} stimulate Na$^+$/H$^+$ exchange across the plasma membrane; however, Gα_{12} requires protein kinase C, whereas Gα_{13} uses a pathway independent of this kinase (Dhanasekaran et al., 1994). Gα_{13} stimulates activity of the Na$^+$/H$^+$ exchangers NHE-1, NHE-2, and NHE-3, but Gα_{12} stimulates only the latter two proteins while inhibiting NHE-1 (Lin et al., 1996). Also, Gα_{12}-mediated regulation of tight junctions and paracellular permeability occurs via a Src-dependent mechanism, whereas the Gα_{13}-mediated response does not require Src (Meyer et al., 2003; Donato et al., 2009). In another example, recruitment of p115RhoGEF to the inner face of the plasma membrane by activated Gα_{13} is dependent on RhoA, whereas recruitment by activated Gα_{12} is refractory to RhoA inhibition (Bhattacharyya et al., 2009). One clue regarding different Hsp90 requirements of the G12/13 proteins has emerged from studies of lipid rafts; Gα_{12}, but not Gα_{13}, localizes to these sphingolipid- and cholesterol-enriched areas, and targeting of Gα_{12} to lipid rafts is sensitive to Hsp90 inhibition (Waheed and Jones, 2002). The different subcellular locations of Gα_{12} and Gα_{13} may facilitate differences in signaling inputs, downstream effectors, and regulators of their respective signaling properties, so that a binding partner such as Hsp90 may be critical for one G12/13 protein but not the other in driving a common downstream response such as SRE activation.

In addition to illuminating target sites for inhibiting Gα_{12}-mediated signaling to SRE-regulated genes, our findings validate the "class-distinctive" methodology (Temple et al., 2010) as a technique that could be extended to other Gα classes to dissect the roles of different binding partners. With the increasing list of proteins that interact with Gα_{12}, Gα_{13}, or other Gα proteins, class-distinctive mutants should be useful for identifying connections between specific Gα-effector interactions and cellular responses mediated by different classes of G proteins.

Authorship Contributions

Participated in research design: Montgomery, Temple, Peters, Tolbert, Rogers, Jones, Meigs.

Conducted experiments: Montgomery, Peters, Tolbert, Smolski, Hamilton, Tagliatela, Rogers, Meigs.

Contributed new reagents or analytic tools: Montgomery, Peters, Booker, Martin, Hamilton, Tagliatela, Rogers, Meigs.

Performed data analysis: Montgomery, Temple, Peters, Tolbert, Rogers, Jones, Meigs.

Wrote or contributed to the writing of the manuscript: Montgomery, Temple, Peters, Tolbert, Rogers, Jones, Meigs.

References

Adarichev VA, Vaiskunaite R, Niu J, Balyasnikova IV, and Voyno-Yasenetskaya TA (2003) Gα13-mediated transformation and apoptosis are permissively dependent on basal ERK activity. *Am J Physiol Cell Physiol* **285**:C922–C934.

Barrett K, Leptin M, and Settleman J (1997) The Rho GTPase and a putative Rho-GEF mediate a signaling pathway for the cell shape changes in Drosophila gastrulation. *Cell* **91**:905–915.

Bhattacharyya R, Banerjee J, Khalili K, and Wedegaertner PB (2009) Differences in Galpha12- and Galpha13-mediated plasma membrane recruitment of p115-RhoGEF. *Cell Signal* **21**:996–1006.

Bhattacharyya R and Wedegaertner PB (2000) Galpha 13 requires palmitoylation for plasma membrane localization, Rho-dependent signaling, and promotion of p115-RhoGEF membrane binding. *J Biol Chem* **275**:14992–14999.

Cabrera-Vera TM, Vanhauwe J, Thomas TO, Medkova M, Preininger A, Mazzoni MR, and Hamm HE (2003) Insights into G protein structure, function, and regulation. *Endocr Rev* **24**:765–781.

Chan AM, Fleming TP, McGovern ES, Chedid M, Miki T, and Aaronson SA (1993) Expression cDNA cloning of a transforming gene encoding the wild-type Gα12 gene product. *Mol Cell Biol* **13**:762–768.

Dhanasekaran N, Prasad MV, Wadsworth SJ, Dermott JM, and van Rossum G (1994) Protein kinase C-dependent and -independent activation of Na+/H+ exchanger by Gα12 class of G proteins. *J Biol Chem* **269**:11802–11806.

Donato R, Wood SA, Saunders I, Gundsambuu B, Yan Mak K, Abbott CA, and Powell BC (2009) Regulation of epithelial apical junctions and barrier function by Galpha13. *Biochim Biophys Acta* **1793**:1228–1235.

Evelyn CR, Wade SM, Wang Q, Wu M, Iñiguez-Lluhí JA, Merajver SD, and Neubig RR (2007) CCG-1423: a small-molecule inhibitor of RhoA transcriptional signaling. *Mol Cancer Ther* **6**:2249–2260.

Friedman EJ, Temple BRS, Hicks SN, Sondek J, Jones CD, and Jones AM (2009) Prediction of protein-protein interfaces on G-protein β subunits reveals a novel phospholipase C β2 binding domain. *J Mol Biol* **392**:1044–1054.

Fromm C, Coso OA, Montaner S, Xu N, and Gutkind JS (1997) The small GTP-binding protein Rho links G protein-coupled receptors and Galpha12 to the serum response element and to cellular transformation. *Proc Natl Acad Sci USA* **94**:10098–10103.

Goulimari P, Knieling H, Engel U, and Grosse R (2008) LARG and mDia1 link Galpha12/13 to cell polarity and microtubule dynamics. *Mol Biol Cell* **19**:30–40.

Grabocka E and Wedegaertner PB (2005) Functional consequences of Gα13 mutations that disrupt interaction with p115RhoGEF. *Oncogene* **24**:2155–2165.

Gu JL, Müller S, Mancino V, Offermanns S, and Simon MI (2002) Interaction of Gα(12) with G α(13) and G α(q) signaling pathways. *Proc Natl Acad Sci USA* **99**:9352–9357.

Guilluy C, Swaminathan V, Garcia-Mata R, O'Brien ET, Superfine R, and Burridge K (2011) The Rho GEFs LARG and GEF-H1 regulate the mechanical response to force on integrins. *Nat Cell Biol* **13**:722–727.

Hajicek N, Kukimoto-Niino M, Mishima-Tsumagari C, Chow CR, Shirouzu M, Terada T, Patel M, Yokoyama S, and Kozasa T (2011) Identification of critical residues in G(α)13 for stimulation of p115RhoGEF activity and the structure of the G(α)13-p115RhoGEF regulator of G protein signaling homology (RH) domain complex. *J Biol Chem* **286**:20625–20636.

Hill CS, Wynne J, and Treisman R (1995) The Rho family GTPases RhoA, Rac1, and CDC42Hs regulate transcriptional activation by SRF. *Cell* **81**:1159–1170.

Hinson JS, Medlin MD, Lockman K, Taylor JM, and Mack CP (2007) Smooth muscle cell-specific transcription is regulated by nuclear localization of the myocardin-related transcription factors. *Am J Physiol Heart Circ Physiol* **292**:H1170–H1180.

Jiang H, Wu D, and Simon MI (1993) The transforming activity of activated Gα12. *FEBS Lett* **330**:319–322.

Jones TL and Gutkind JS (1998) Galpha12 requires acylation for its transforming activity. *Biochemistry* **37**:3196–3202.

Juneja J and Casey PJ (2009) Role of G12 proteins in oncogenesis and metastasis. *Br J Pharmacol* **158**:32–40.

Kelly P, Casey PJ, and Meigs TE (2007) Biologic functions of the G12 subfamily of heterotrimeric G proteins: growth, migration, and metastasis. *Biochemistry* **46**:6677–6687.

Kelly P, Moeller BJ, Juneja J, Booden MA, Der CJ, Daaka Y, Dewhirst MW, Fields TA, and Casey PJ (2006a) The G12 family of heterotrimeric G proteins promotes breast cancer invasion and metastasis. *Proc Natl Acad Sci USA* **103**:8173–8178.

Kelly P, Stemmle LN, Madden JF, Fields TA, Daaka Y, and Casey PJ (2006b) A role for the G12 family of heterotrimeric G proteins in prostate cancer invasion. *J Biol Chem* **281**:26483–26490.

Kozasa T and Gilman AG (1995) Purification of recombinant G proteins from Sf9 cells by hexahistidine tagging of associated subunits: characterization of α 12 and inhibition of adenylyl cyclase by α z. *J Biol Chem* **270**:1734–1741.

Kreutz B, Yau DM, Nance MR, Tanabe S, Tesmer JJG, and Kozasa T (2006) A new approach to producing functional G α subunits yields the activated and deactivated structures of Gα(12/13) proteins. *Biochemistry* **45**:167–174.

Lin X, Voyno-Yasenetskaya TA, Hooley R, Lin CY, Orlowski J, and Barber DL (1996) Galpha12 differentially regulates Na+-H+ exchanger isoforms. *J Biol Chem* **271**:22604–22610.

Medjkane S, Perez-Sanchez C, Gaggioli C, Sahai E, and Treisman R (2009) Myocardin-related transcription factors and SRF are required for cytoskeletal dynamics and experimental metastasis. *Nat Cell Biol* **11**:257–268.

Medlin MD, Staus DP, Dubash AD, Taylor JM, and Mack CP (2010) Sphingosine 1-phosphate receptor 2 signals though leukemia-associated RhoGEF (LARG), to promote smooth muscle cell differentiation. *Arterioscler Thromb Vasc Biol* **30**:1779–1786.

Meigs TE, Juneja J, DeMarco CT, Stemmle LN, Kaplan DD, and Casey PJ (2005) Selective uncoupling of Gα12 from Rho-mediated signaling. *J Biol Chem* **280**:18049–18055.

Meyer TN, Hunt J, Schwesinger C, and Denker BM (2003) Galpha12 regulates epithelial cell junctions through Src tyrosine kinases. *Am J Physiol Cell Physiol* **285**:C1281–C1293.

Miller RT, Masters SB, Sullivan KA, Beiderman B, and Bourne HR (1988) A mutation that prevents GTP-dependent activation of the α chain of Gs. *Nature* **334**:712–715.

Nakamura S, Kreutz B, Tanabe S, Suzuki N, and Kozasa T (2004) Critical role of lysine 204 in switch I region of Galpha13 for regulation of p115RhoGEF and leukemia-associated RhoGEF. *Mol Pharmacol* **66**:1029–1034.

Offermanns S, Mancino V, Revel JP, and Simon MI (1997) Vascular system defects and impaired cell chemokinesis as a result of Galpha13 deficiency. *Science* **275**:533–536.

Oldham WM and Hamm HE (2008) Heterotrimeric G protein activation by G-protein-coupled receptors. *Nat Rev Mol Cell Biol* **9**:60–71.

Pai KS and Cunningham DD (2002) Geldanamycin specifically modulates thrombin-mediated morphological changes in mouse neuroblasts. *J Neurochem* **80**:715–718.

Parks S and Wieschaus E (1991) The Drosophila gastrulation gene concertina encodes a Gα-like protein. *Cell* **64**:447–458.

Peterson LB and Blagg BS (2009) To fold or not to fold: modulation and consequences of Hsp90 inhibition. *Future Med Chem* **1**:267–283.

Ren XD, Kiosses WB, and Schwartz MA (1999) Regulation of the small GTP-binding protein Rho by cell adhesion and the cytoskeleton. *EMBO J* **18**:578–585.

Rogers SL and Rogers GC (2008) Culture of Drosophila S2 cells and their use for RNAi-mediated loss-of-function studies and immunofluorescence microscopy. *Nat Protoc* **3**:606–611.

Samant RS, Clarke PA, and Workman P (2012) The expanding proteome of the molecular chaperone HSP90. *Cell Cycle* **11**:1301–1308.

Shi CS, Sinnarajah S, Cho H, Kozasa T, and Kehrl JH (2000) G13α-mediated PYK2 activation. PYK2 is a mediator of G13α-induced serum response element-dependent transcription. *J Biol Chem* **275**:24470–24476.

Sternweis PC, Carter AM, Chen Z, Danesh SM, Hsiung YF, and Singer WD (2007) Regulation of Rho guanine nucleotide exchange factors by G proteins. *Adv Protein Chem* **74**:189–228.

Suzuki N, Hajicek N, and Kozasa T (2009) Regulation and physiological functions of G12/13-mediated signaling pathways. *Neurosignals* **17**:55–70.

Temple BRS, Jones CD, and Jones AM (2010) Evolution of a signaling nexus constrained by protein interfaces and conformational states. *PLOS Comput Biol* **6**:e1000962.

Uetrecht AC and Bear JE (2009) Golgi polarity does not correlate with speed or persistence of freely migrating fibroblasts. *Eur J Cell Biol* **88**:711–717.

Vaiskunaite R, Kozasa T, and Voyno-Yasenetskaya TA (2001) Interaction between the Gα subunit of heterotrimeric G(12) protein and Hsp90 is required for Gα(12) signaling. *J Biol Chem* **276**:46088–46093.

Vara Prasad MV, Shore SK, and Dhanasekaran N (1994) Activated mutant of G alpha 13 induces Egr-1, c-fos, and transformation in NIH 3T3 cells. *Oncogene* **9**:2425–2429.

Vázquez-Prado J, Miyazaki H, Castellone MD, Teramoto H, and Gutkind JS (2004) Chimeric G α i2/G α 13 proteins reveal the structural requirements for the binding and activation of the RGS-like (RGL)-containing Rho guanine nucleotide exchange factors (GEFs) by G α 13. *J Biol Chem* **279**:54283–54290.

Waheed AA and Jones TLZ (2002) Hsp90 interactions and acylation target the G protein Galpha 12 but not Galpha 13 to lipid rafts. *J Biol Chem* **277**:32409–32412.

Wang DZ, Li S, Hockemeyer D, Sutherland L, Wang Z, Schratt G, Richardson JA, Nordheim A, and Olson EN (2002). Potentiation of serum response factor activity by a family of myocardin-related transcription factors. *Proc Natl Acad Sci USA* **99**:14855–14860.

Worzfeld T, Wettschureck N, and Offermanns S (2008) G(12)/G(13)-mediated signalling in mammalian physiology and disease. *Trends Pharmacol Sci* **29**:582–589.

Xu N, Voyno-Yasenetskaya T, and Gutkind JS (1994) Potent transforming activity of the G13 α subunit defines a novel family of oncogenes. *Biochem Biophys Res Commun* **201**:603–609.

Yamaguchi Y, Katoh H, and Negishi M (2003) N-terminal short sequences of α subunits of the G12 family determine selective coupling to receptors. *J Biol Chem* **278**:14936–14939.

Yau DM, Yokoyama N, Goshima Y, Siddiqui ZK, Siddiqui SS, and Kozasa T (2003) Identification and molecular characterization of the Gα12-Rho guanine nucleotide exchange factor pathway in Caenorhabditis elegans. *Proc Natl Acad Sci USA* **100**:14748–14753.

Yu W, Ritchie BJ, Su X, Zhou J, Meigs TE, and Denker BM (2011) Identification of polycystin-1 and Gα12 binding regions necessary for regulation of apoptosis. *Cell Signal* **23**:213–221.

Zhu D, Tate RI, Ruediger R, Meigs TE, and Denker BM (2007) Domains necessary for Galpha12 binding and stimulation of protein phosphatase-2A (PP2A): Is Galpha12 a novel regulatory subunit of PP2A? *Mol Pharmacol* **71**:1268–1276.

Address correspondence to: Thomas E. Meigs, Department of Biology, University of North Carolina at Asheville, CPO 2040, One University Heights, Asheville, NC 28804. E-mail: tmeigs@unca.edu